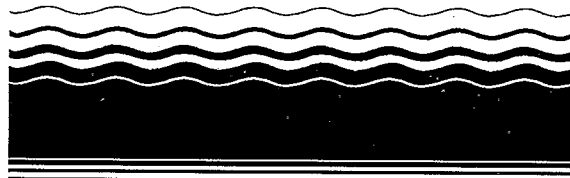




SITE

**SUPERFUND INNOVATIVE
TECHNOLOGY EVALUATION**



Emerging Technology Summary

Integration of Photocatalytic Oxidation with Air Stripping of Contaminated Aquifers

Rajnish Changrani, Gregory B. Raupp, and Craig Turchi

In a recently completed test program, bench-scale laboratory studies at Arizona State University (ASU) in Tempe, AZ, and pilot-scale studies in a simulated field-test situation at Zentox Corporation in Ocala, FL, were performed to evaluate the integration of gas-solid ultraviolet (UV) photocatalytic oxidation (PCO) with air stripping of an aquifer contaminated with chlorinated volatile organic compounds (VOCs). Chlorinated ethylenes such as trichloroethylene (TCE) can be destroyed in a wide process window, although chlorinated ethanes such as trichloroethane (TCA) are nonreactive. Water vapor significantly inhibits the chlorinated ethylene destruction rate. For this reason, PCO units should be placed downstream of a dehumidification unit located between air strippers and the PCO unit, with targeted reduction of the relative humidity in the contaminated air stream to less than 50%. Principal carbon-containing products of PCO identified experimentally at the bench scale include carbon dioxide, carbon monoxide, and phosgene (COCl_2). Failure to close carbon mass balances under some process conditions suggests that not all byproducts were identified. Further studies are needed in this area. A panel

bed was identified as the preferred photoreactor configuration. This unit is characterized by simplicity of construction, ease of maintenance, and high UV photon utilization efficiency.

This Emerging Technology Summary was developed by EPA's National Risk Management Research Laboratory, Cincinnati, OH, to announce key findings of the research project that is fully documented in a separate report of the same title (see Project Report ordering information at back).

Introduction

Contamination of drinking water aquifers with volatile chlorinated organic solvents is a widespread problem across industrialized areas of the U.S. The global objective of this work was to evaluate the integration of gas-solid ultraviolet (UV) photocatalytic oxidation (PCO) downstream of an air stripper unit as a technology for cost-effectively treating water pumped from an aquifer contaminated with chlorinated volatile organic compounds (VOCs). The photocatalytic oxidation process integrated with air stripping is shown schematically in Figure 1. In this configuration, the air stripper off-gases are fed directly to the PCO reactor without pretreatment. In the



continuous flow PCO reactor, the contaminated air stream contacts the surface of a near-ultraviolet irradiated titania (TiO_2) catalyst, causing photochemical destruction of the contaminants at or near room temperature. Exhaust gas from the PCO reactor is fed to a dry scrubber for removal of HCl and Cl_2 generated during the oxidation of chlorinated solvents.

The *primary* objectives of this research project were as follows:

- Define the optimum gas residence time, catalyst characteristics, UV light intensity, and photoreactor configuration that achieves greater than 95% destruction of the primary VOCs (trichloroethylene and trichloroethane) in air stripper off-gases.
- Characterize the overall performance of the integrated air stripper/PCO process by quantifying contaminant destruction during short-term transients generated by air stripper startup, shutdown, and upsets, and by quantifying destruction performance over an extended test period.

The *secondary* objectives of this project included the following:

- Quantify catalyst lifetime independent of factors related to integration of the PCO unit with an air stripper.
- Identify reaction byproducts and conditions that inhibit or enhance their formation.

Most of these objectives were successfully achieved through bench-scale and pilot-scale controlled testing described in the body of this report. The first objective was met through the following strategy. Statistically designed experiments enabled efficient process performance characterization as a function of key process variables. The derived empirical response surface models allowed prediction of conditions for which high VOC destruction efficiency could be achieved. These predictions were subsequently confirmed in a long-term bench-scale test and in several short-term pilot-scale tests. Because we were unable to obtain actual field test data, the second primary objective listed above could not be achieved.

Experimental Methods

The bench-scale PCO system at ASU is shown schematically in Figure 2. A CO_2 -free synthetic air mixture contaminated to a predetermined level is prepared by continuously mixing gases from pressurized gas cylinders using mass flow controllers (mfc). Water vapor is added to the feed flow by a separate nitrogen flow through a saturator. The humid, contaminated air is fed to an annular photoreactor incorporat-

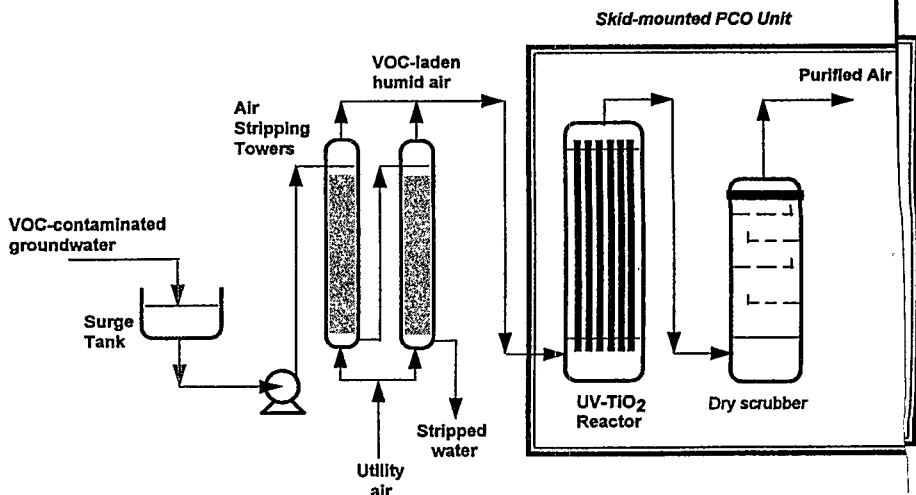


Figure 1. Integrated air stripping with photocatalytic oxidation process.

ing a 1.5" OD 20 W UV black lamp in a 2.25" ID glass tube. The annular space is filled with titania-coated packing; bed length is 90 cm. Ultraviolet light fluxes at the lamp and at the reactor outer wall were measured with a Minolta integrating photometer.

The system incorporates three in-line sensors (Sens1, Sens2 and Sens3) and three discrete sampling locations (Sam1, Sam2 and Sam3). Sam1 and Sam2 are automatic multiple port GC sampling valves which send a well-defined volume of gas to one of two columns in the Varian 3700 GC for VOC and carbon dioxide analysis, respectively. The third sampling location (Sam3) allows gas samples to be withdrawn for off-line analysis by gas detection tubes. Sens1 is an in-line relative humidity sensor (Vaisala). Sens2 and Sens3 are in-line electrochemical sensors for HCl (Detcon) and CO (Sierra) measurement, respectively. Flow, temperature and pressure measuring devices are also included as indicated in the figure. Measurements are recorded using automatic data acquisition driven by a Hewlett-Packard 486 processor based PC.

Testing Procedures

For a given performance evaluation run, gas flows are set and stabilized and the feed gas is analyzed with the sensors and GCs until a steady reading is achieved. At this point, the UV lamps are illuminated, and the reactor outlet is regularly analyzed. Once steady operating conditions are achieved (typically several hours with fresh catalyst beds, several minutes with conditioned beds), measurements are recorded for several more hours. It is these average steady state values (usually six

to eight points taken over two hours) that are reported.

Three unique sets of experiments were run. Set 1 was designed to characterize the performance of the bench-scale unit under process conditions that are representative of those found in the field at the target industrial field site is currently being pumped and treated by a 660 gallons per minute remediation plant employing air stripping and carbon bed adsorption of the stripper off-gases. In the planned field test, the PCO unit would have been employed to treat a slipstream of the air stripper off-gases. The expected total VOC concentration ranges from 10 to 18 ppmv, with typically two-thirds of the total attributed to TCE. An in-line dehumidifier reduces the relative humidity (RH) in the off-gases to about 50% upstream of the carbon beds.

Process characterization was efficiently achieved by employing statistical design of experiments (DOE) surface response methodology (SRM). Table 1 summarizes the independent process variables and levels. The chosen $1/2$ fraction of a 2^5 factorial design augmented with axial runs and center point replicates, or "face centered cubic" design, provides a complete response surface and has a reasonably stable variance over a large portion of the design region.

Set 2 is designed to efficiently characterize the performance of the bench-scale unit for conversion of complex contaminant mixtures. Set 3 experiments were designed to test the long-term stability of the photocatalyst in a reactive environment.

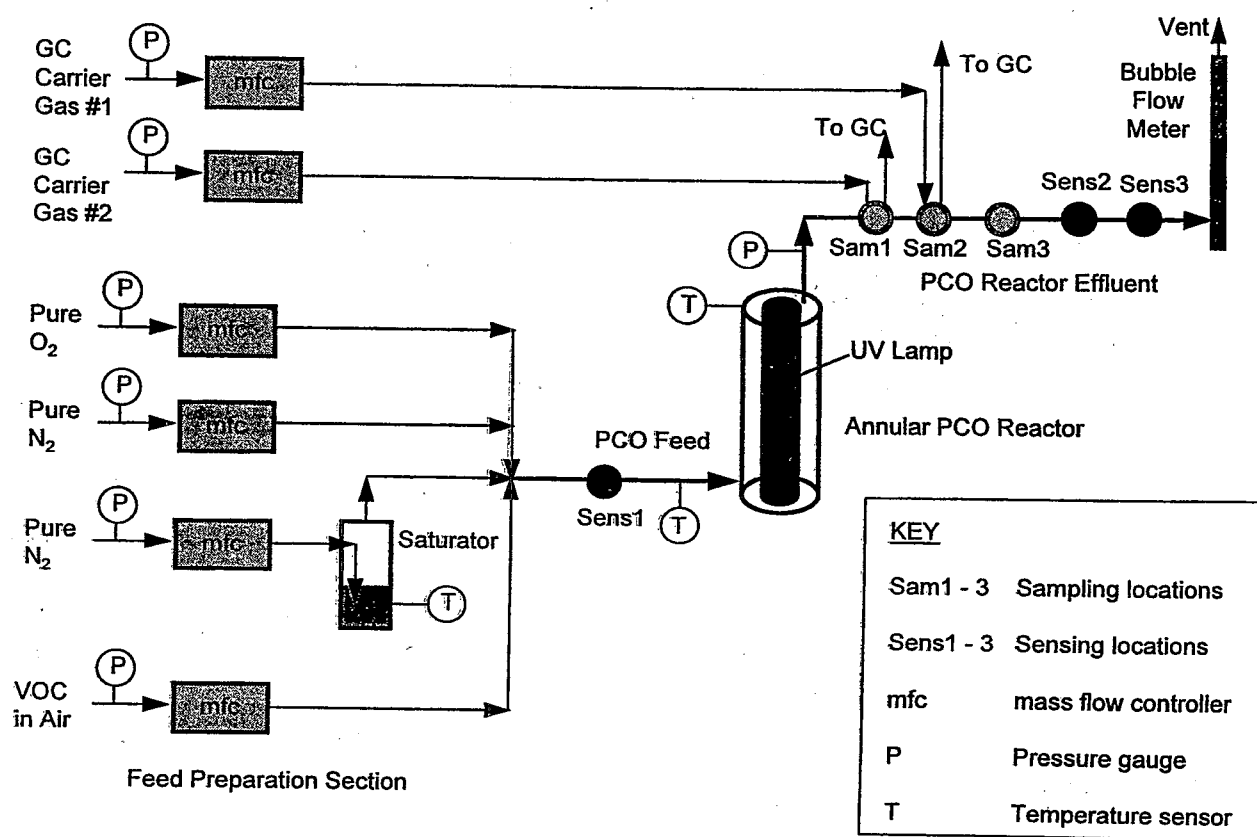


Figure 2. Bench-scale photocatalytic oxidation apparatus.

Table 1. Process Parameters and Levels

| Factor | Code | Low (-1) | Center (0) | High (+1) |
|--|------|----------|------------|-----------|
| Total inlet VOC concentration (ppm _v) | A | 10 | 20 | 30 |
| Relative Humidity (%) | B | 20 | 50 | 80 |
| UV Intensity _{wall} (mW/cm ²) | C | 0.5 | 2.0 | 3.5 |
| Temperature (°C) | D | 40 | 60 | 80 |
| Residence time (s) | E | 0.5 | 1.0 | 1.5 |

The principal measured responses are conversion X_{VOC} of the VOC and selectivity S_{CO_2} of the reaction towards producing CO_2 . Conversion is a direct measure of destruction efficiency, while the selectivity is a measure of the percentage of the VOCs destroyed that are converted to the desired complete combustion product carbon dioxide.

Results and Discussion

Set 1 Results Under the conditions of these experiments, TCA conversion is essentially negligible, with measured values

ranging between about 2 and 6%. For purposes of brevity, subsequent DOE models for VOC conversion described below and the accompanying discussion are for TCE conversion only. Trichloroethylene conversion data are described by the following quadratic model:

$$X_{VOC} = 111.02 - 0.22 \cdot VOC - 2.81 \cdot RH + 9.02 \cdot UV - 0.23 \cdot T + 42.0 \cdot \tau - 15.11 \cdot \tau^2 - 0.07 \cdot RH \cdot UV + 0.008 \cdot RH \cdot T$$

where VOC = VOC concentration (ppm_v), RH = Relative Humidity (%), UV = UV intensity (mW/cm²), T = Temperature (K), and τ = residence time (s). The model reveals that all five independent factors are significant. The three-dimensional response surfaces are shown in Figures 3 and 4. Increasing residence time and UV intensity increase VOC conversion, whereas increasing RH decreases VOC conversion. Inhibition of the TCE photocatalytic oxidation rate by water vapor is a well-established phenomenon first reported by our laboratory.

The following linear model adequately describes the observed selectivity behavior:

$$S_{CO_2} = -23.90 - 1.61 \cdot VOC - 0.19 \cdot RH + 3.93 \cdot UV + 0.43 \cdot T - 12.51 \cdot \tau + 0.0002 \cdot VOC \cdot UV \cdot T$$

where variables are as defined previously. Increasing VOC concentration decreases selectivity, while increasing light intensity (UV) and increasing temperature (T) increase selectivity. In addition, there is an interaction among VOC concentration, UV and T. The magnitude of the interaction

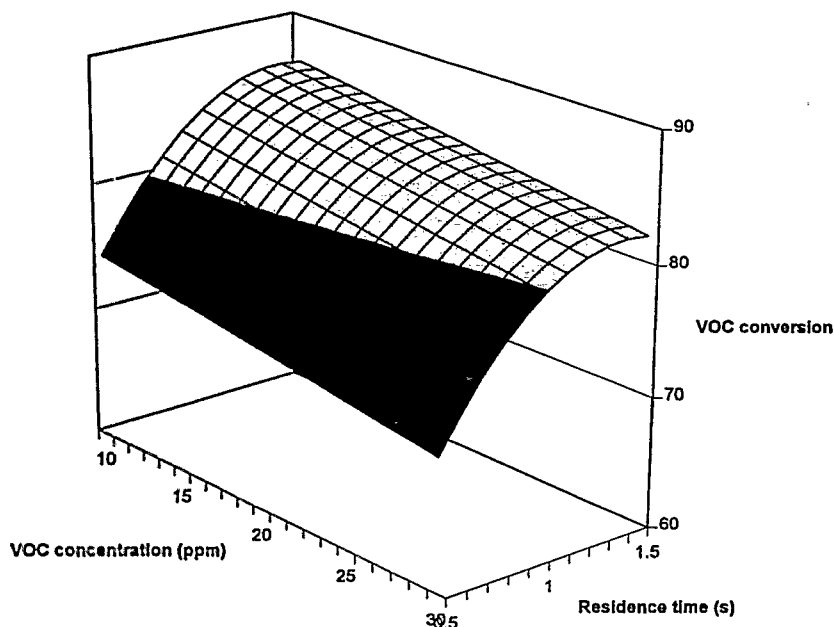


Figure 3. Response surface for VOC conversion versus residence time and inlet VOC concentration. Twenty percent RH, 3.5 mW/cm² UV intensity, 40°C.

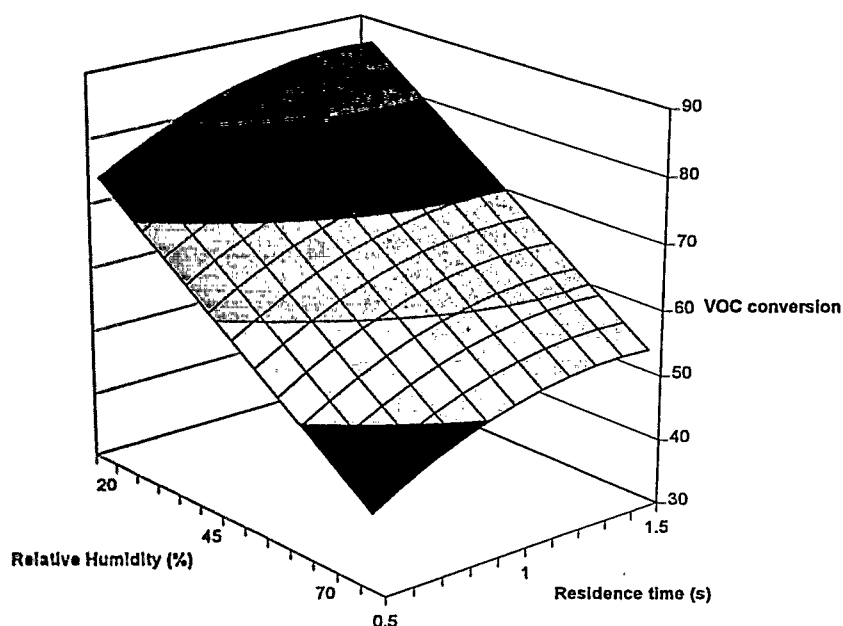


Figure 4. Response surface for VOC conversion versus residence time and RH. Ten ppm_v VOC concentration, 3.5 mW/cm² UV intensity, 40°C.

term, while statistically significant, is small relative to the main factor effects. The main selectivity responses can be explained within the framework of a surface-mediated, free-radical sequential oxidation mechanism. In this model, hydroxyl radicals created through UV excitation of the

titania photocatalyst initiate oxidative attack on adsorbed VOCs to create VOC radicals. The radical sites are then attacked by oxygen to create peroxy radicals. These reactive peroxy radicals readily decompose to produce partial oxidation products on the catalyst surface. This se-

ries hydroxyl radical attack, oxygen addition sequence continues until complete combustion products are produced. We hypothesize that TCE is first oxidized to dichloroacetaldehyde, then to dichloroacetic acid, and ultimately to chlorinated formic acid intermediates. Under dry conditions ($\leq 10\%$ RH), hydroxyl radicals may not be the primary initiator of oxidation, and an alternative reaction path through phosgene becomes dominant. With increasing relative humidity, the production of phosgene and other undesirable intermediates decreases. For sufficiently high humidity ($>40\text{-}50\%$) and residence time, essentially complete conversion to carbon dioxide is observed.

Assuming typical Langmuir-Hinshelwood-Hougen-Watson (LHHW) reaction kinetics determine the TCE destruction rate, increasing TCE concentration should increase the average surface coverage by TCE. For otherwise fixed conditions, the production rate of reactive hydroxyl radicals will be essentially the same. At steady state, there will therefore be relatively fewer hydroxyls to attack adsorbed partial oxidation intermediates, leading to a reduced integrated selectivity to CO₂. A similar argument can be posed to explain the UV dependence. With increasing UV intensity, the production rate of hydroxyl radicals increases. A relatively greater number of hydroxyls will be available to attack partial oxidation intermediates, leading to an increased integrated selectivity to CO₂.

No VOCs other than TCE and TCA were observed in the GC chromatograms. Carbon monoxide levels were between 0.5 to 1.5 ppm_v for all experimental runs. Molecular chlorine (Cl₂) and phosgene (COCl₂) levels were observed at levels <0.2 ppm_v; no significant hydrogen chloride was detected. The calculated carbon mass balances for the Set 1 experimental runs range from ca. 60 to 100%. In general, highest percent closures were obtained for low inlet VOC concentration. Low inlet TCE concentrations also favor higher selectivity. Lack of closure could not be attributed to inaccuracy in CO₂ measurements but is instead most likely due to non-detect of volatile partial oxidation products including, but not necessarily limited to, dichloroacetyl chloride. A Cl atom balance is not reported since, except for unconverted TCE, only very small amounts of chlorine-containing compounds were detected in the reactor outlet for all runs. It is likely that chlorine buildup on the catalyst surface is responsible for the low levels of chlorine-containing compounds detected in the reactor effluent.

Set 2 Results At the target Superfund site, co-contaminant or secondary VOCs present along with the primary VOCs are 1,1-dichloroethylene, cis 1,2-dichloroethylene, vinyl chloride, tetrachloroethylene (also known as perchloroethylene), and 1,2-dichlorobenzene. Each of these co-contaminants is present in varying amounts depending on air stripper operation, but under no circumstance have levels higher than 1 ppm_v been detected. A mixture experimental design in which the chlorinated ethylenes were lumped together to create a "secondary chlorinated ethylenes" pseudocomponent was employed. This strategy yields the following three-component mixture: trichloroethylene (mole fraction x_1), secondary chlorinated ethylenes (mole fraction x_2), and 1,2-dichlorobenzene (mole fraction x_3). The initial concentrations for each of the chlorinated VOCs in the lumped secondary chlorinated ethylenes category were held in the same ratio for all experiments, at levels designed to approximate the average ratios found at the Superfund site.

A 3² factorial mixture experiment was designed to capture the maximum pseudocomponent ratios $R_1 = x_1 / x_2$ and $R_2 = x_1 / x_3$ expected at the Superfund site. Table 2 summarizes these ratios and the corresponding pseudo mole fractions of the three pseudocomponents for the nine experimental runs performed in this set. Other process conditions were fixed at representative values as follows: TCE inlet concentration = 10 ppm_v, RH = 20%, UV Intensity = 3.5 mW/cm², Temperature = 40°C., and residence time = 0.5 s. These process values were chosen to yield a TCE conversion that was reasonably high (order of 70%) but not so high (i.e., >95%) that conversion sensitivity to the presence of co-contaminants would be masked by poor measurement statistics.

A statistical analysis of the experimental data revealed that nearly the entire

sum of squares is explained by the sum of squares for the mean, i.e., that the effect of the co-contaminants on TCE conversion is *not* statistically significant. Selectivity depends on the pseudocomponent ratios according to the following quadratic model:

$$S_{CO_2} = -39.19 + 10.69 \cdot R_1 + 9.23 \cdot R_2 + 0.71 \cdot R_1^2 - 0.26 \cdot R_2^2 - 0.525 \cdot R_1 \cdot R_2$$

Figure 5 shows this response visually. The response shows a complex dependence on the pseudocomponent ratios. As the ratio (R_1) of TCE to secondary chlorinated ethylenes increases, selectivity increases regardless of the chlorobenzene level. The increase is most dramatic at the lowest ratio of TCE to chlorobenzene. The Selectivity tends to go through a broad maximum as the ratio (R_2) of TCE to chlorobenzene increases, with the location of the maximum shifting to lower R_2 ratios as the ratio of TCE to secondary chlorinated ethylenes increases.

Carbon mass balance closures range from ca. 60 to near 100% (basically the same range observed for the factorial experiments in Set 1). As for Set 1, a chlorine atom balance is not reported since essentially no chlorine-containing compounds other than those found in unconverted VOCs were detected in the reactor outlet for all runs.

Set 3 Results These experiments were designed to test the long-term stability of the photocatalyst in a reactive environment. Process conditions were chosen so that high TCE conversion (>95%) and selectivity (100%) were obtained during the initial stages of the run. To simplify gas analysis, TCE was the only VOC in the contaminated air stream. A freshly-prepared catalyst bed was employed.

Over the course of the first six days of operation, TCE conversion held steady at greater than 95%, while Selectivity was constant at approximately 100%. The C mass balance was essentially closed in all measurements ($\approx 100\%$). The Cl atom mass balance was only about 3-4%. After six days on stream, a dramatic change in performance was observed. The Cl atom balance closure jumped to the 70-80% closure range. This improved closure is associated with the appearance of substantial concentrations of HCl and Cl₂, as well as lesser amounts of COCl₂. Selectivity fell below 100% at this point as a portion of the inlet C appeared in the COCl₂ byproduct. Over the remainder of the run, the TCE conversion gradually fell, although it remained above 90% over the entire duration. The selectivity also gradually fell, although it remained above 95%. The findings in this experiment are consistent with a model in which the fresh

Table 2. Mixture Experimental Design

| Run ID | R_1 | R_2 | X_1 | X_2 | X_3 |
|--------|-------|-------|-------|-------|-------|
| 1 | 2 | 6 | 0.60 | 0.30 | 0.10 |
| 2 | 4 | 6 | 0.70 | 0.18 | 0.12 |
| 3 | 6 | 6 | 0.75 | 0.13 | 0.12 |
| 4 | 2 | 11 | 0.63 | 0.31 | 0.06 |
| 5 | 4 | 11 | 0.74 | 0.19 | 0.07 |
| 6 | 6 | 11 | 0.80 | 0.13 | 0.07 |
| 7 | 2 | 16 | 0.64 | 0.32 | 0.04 |
| 8 | 4 | 16 | 0.76 | 0.19 | 0.05 |

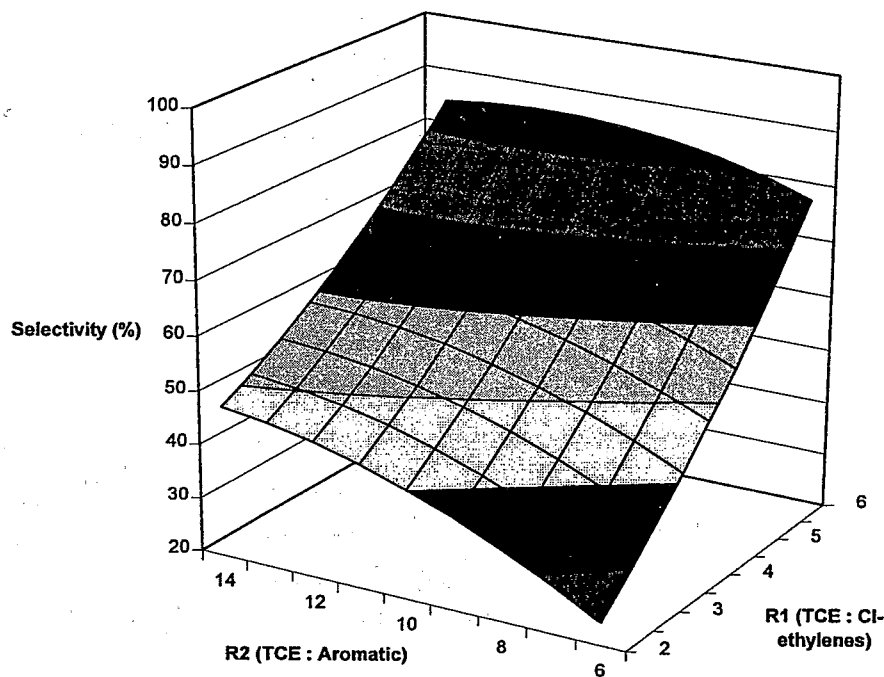


Figure 5. Influence of pseudocomponent ratios R_1 and R_2 on selectivity.

surface becomes chlorinated as TCE is dechlorinated and oxidized in the PCO process. Initially this deposited Cl is non-volatile and an inventory of adsorbed Cl builds up on the surface as TCE-containing air is treated. At the point of Cl atom saturation on the surface, TCE conversion continues but chlorine produced subsequently is volatile, appearing in the gas phase as HCl, Cl₂, and COCl₂.

Pilot-Scale Experiments

A commercial scale reactor should be designed to achieve high integrated photon utilization efficiencies, while providing low pressure drop, high throughput operation in a reasonably compact physical configuration. The preferred reactor configuration is a key technical issue addressed in this research. Figure 6 compares the two principal reactor configurations tested in this research project. Configuration 1 is the packed bed design, in which a cylindrical photoreactor containing a number of equally-spaced parallel UV lamps is packed with a catalyst-coated support material. The air flows parallel to the lamps that irradiate the sup-

ported catalyst. Configuration 2 is panel bed design, in which a rectangular duct-shaped photoreactor contains a number of alternating UV lamp banks and a removable panel-type catalyst support material. In this design, the air flows perpendicular to the lamps that irradiate the panels.

Set 1: Reactor Configuration 1 Table 3 summarizes TCE conversion performance for a set of controlled pilot-scale runs at Zentox's production facility with Reactor Configuration 1. Note that the temperature reported refers to the ambient air temperature, not the temperature of the reactor, which should be substantially higher (20 to 40°C.) due to thermal energy dissipation of the UV lamps. Inhibition of the VOC conversion rate by the presence of water vapor is substantial at the pilot-scale as evidenced by a comparison of Run 1 with Run 2, and by a comparison of Run 7 with Run 8. The inhibition effect appears to be more severe at the lower TCE concentrations (Runs 1 and 2). Second, higher destruction efficiencies are achieved for lower air flow rates (compare Runs 3 and 4). This

behavior is essentially a residence time effect expected for rate-based processes.

Although this reactor configuration yielded acceptable performance characteristics with respect to throughput and light utilization, the packed bed design used a support material that was difficult to coat with catalyst, and the loosely packed bed was cumbersome to exchange if a catalyst replacement was necessary or desired. Moreover, because the support was organic polymer based, it tended to degrade under UV irradiation. An improved reactor configuration was therefore designed, constructed and tested based on experience gained in the laboratory and in these pilot-scale tests.

Set 2: Reactor Configuration 2 Table 4 summarizes TCE conversion performance for a set of short-term, controlled pilot-scale runs at Zentox's production facility with a layered, perpendicular flow PCO reactor (Reactor Configuration 2). This design employed consecutive, alternating banks of lamps and catalyst-coated panels.

In a general qualitative sense, this reactor configuration exhibits the same per-

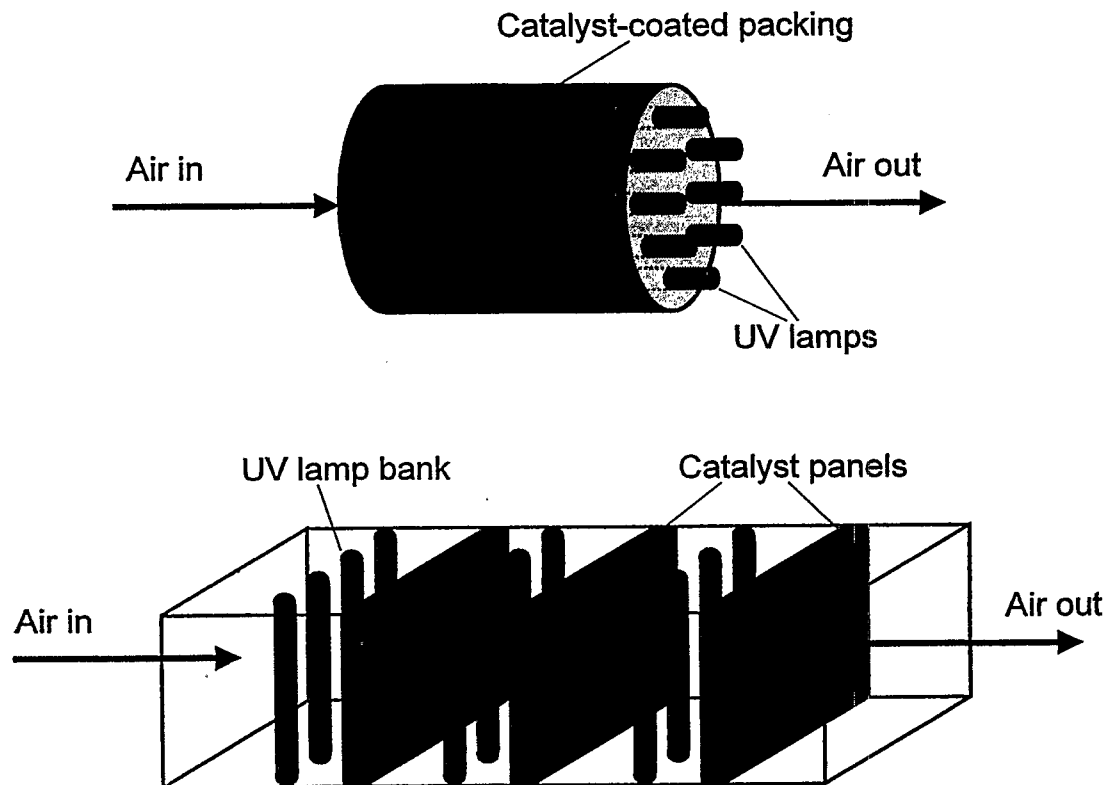


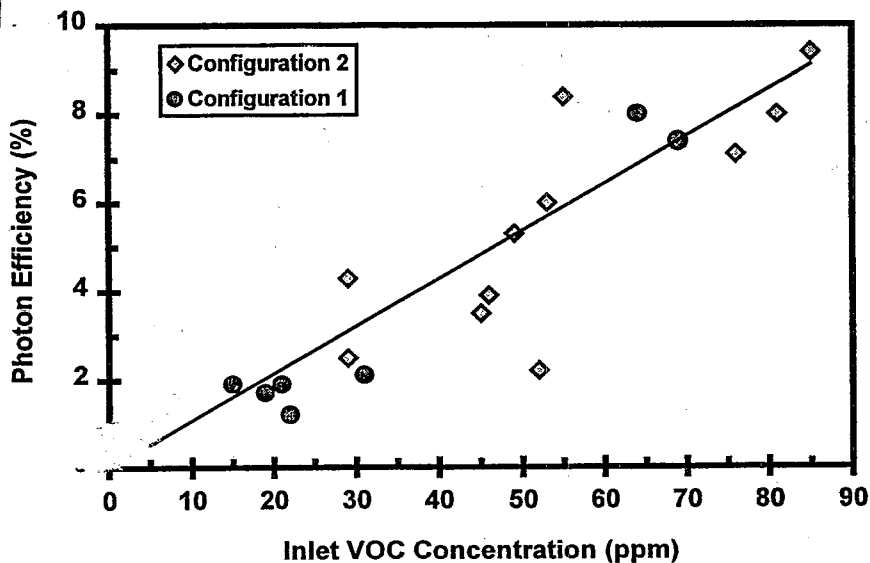
Figure 6. Photocatalytic oxidation reactor configurations. Configuration 1 (top) is a packed bed design, and Configuration 2 (bottom) is a panel bed design.

Table 3. TCE Conversion Results for Reactor Configuration 1

| Run No. | UV Lamps | Air Flow (scfm) | Temp. (°C.) | TCE (ppm _v) | RH (%) | Conversion (%) | Photon Efficiency (%) |
|---------|----------|-----------------|-------------|-------------------------|--------|----------------|-----------------------|
| 1 | 22 | 28 | 21 | 22 | 76 | 55 | 1.2 |
| 2 | 22 | 28 | 33 | 19 | 23 | 90 | 1.7 |
| 3 | 22 | 28 | 24 | 21 | 45 | 90 | 1.9 |
| 4 | 22 | 20 | 24 | 31 | 45 | 96 | 2.1 |
| 5 | 22 | 38 | 24 | 15 | 44 | 90 | 1.9 |
| 6 | 0 | 39 | 22 | 67 | 68 | 5 | — |
| 7 | 22 | 39 | 22 | 69 | 68 | 77 | 7.4 |
| 8 | 22 | 39 | 32 | 64 | 25 | 90 | 8.0 |

Table 4. TCE Conversion Results for Reactor Configuration 2

| Run No. | UV Lamps | Air Flow (scfm) | Inlet Temp. (°C.) | TCE Inlet (ppm _v) | RH (%) | TCE Conversion (%) | Photon Efficiency (%) |
|---------|----------|-----------------|-------------------|-------------------------------|--------|--------------------|-----------------------|
| 10 | 18 | 28 | 28 | 85 | 24 | 90 | 9.4 |
| 11 | 18 | 43 | 29 | 55 | 24 | 81 | 8.4 |
| 12 | 18 | 27 | 23 | 81 | 47 | 85 | 8.0 |
| 13 | 18 | 43 | 24 | 29 | 45 | 77 | 4.3 |
| 14 | 18 | 22 | 24 | 29 | 43 | 89 | 2.5 |
| 15 | 18 | 41 | 26 | 53 | 60 | 62 | 6.0 |
| 16 | 18 | 25 | 26 | 76 | 45 | 87 | 7.1 |
| 17 | 46 | 50 | 29 | 45 | 40 | 91 | 3.5 |
| 18 | 46 | 50 | 32 | 46 | 20 | 99 | 3.9 |
| 19 | 50 | 75 | 27 | 52 | 70 | 36 | 2.2 |
| 20 | 50 | 75 | 41 | 49 | 21 | 92 | 5.3 |

**Figure 7.** Integrated photon efficiency versus inlet TCE concentration for the two pilot reactor configurations.

formance behavior as the first reactor configuration. A direct performance comparison of the two reactor configurations is not possible since the reactors were not tested under identical conditions of flow rate, VOC concentration, relative humidity, and temperature. Apparent photon efficiency is a performance metric adopted by PCO equipment suppliers to allow comparison of the inherent energy efficiencies of different photoreactor designs. Figure 7 is a visual comparison of the effective photon utilization in each configuration versus inlet VOC concentration. Although there are significant run-to-run variations in process parameters, the figure shows that the two designs behave roughly the same at equivalent inlet VOC concentrations in terms of effective photon utilization. The lower fabrication cost and simpler maintenance make the second configuration a superior design.

Conclusions

Controlled testing of two pilot-scale reactor systems revealed that they exhibit qualitatively similar performance characteristics: Integrated photon utilization efficiencies depend on inlet TCE concentration, with higher efficiencies observed for higher inlet concentration. The primary advantages of the second configuration lie in ease of fabrication and maintenance. In particular, the second or panel configuration utilizes a catalyst support that is simple to produce, and that allows simple, rapid installation or exchange of the active catalyst loaded panels.

Based on the results of our bench-scale studies, we can make the following conclusions on PCO process performance for the target application:

- Although a large process conditions window exists for which TCE can be destroyed, trichlorethane (TCA) is nonreactive. Thus, PCO as presently employed is not a viable technology for treating TCA-contaminated air streams.
- Increasing incident UV light intensity and mean gas residence time increase TCE conversion. The quantitative operating window (combination of process conditions) required to yield 95% TCE destruction can be predicted through an empirical response surface model. In general, UV intensities greater than 3.5 mW/cm² and residence times greater than 2.5 s will yield greater than 95% TCE destruction.
- Water vapor significantly inhibits the VOC destruction rate for chlorinated

ethylenes such as TCE. For this reason, PCO units should be placed downstream of a dehumidification unit located between air strippers and the PCO unit. For high VOC conversion operation in the PCO unit, these dehumidifiers should reduce the RH to less than 50%.

- Principal carbon-containing products of PCO identified experimentally at the bench scale include CO₂, CO, and phosgene (COCl₂). Failure to close carbon mass balances under some conditions suggests that not all byproducts were identified.
- The presence of secondary chlorinated ethylenes and chlorobenzene did not significantly affect the conversion of the primary VOC TCE. However, selectivity to the desired complete combustion product carbon dioxide decreased with increasing co-contaminant concentration, suggesting that the presence of the co-contaminants enhanced the production of undesirable partial oxidation products.

- TCE destruction activity could be maintained for up to thirty days on stream. Results suggested that chlorine atoms build up on a fresh catalyst surface during an initial period of operation until the surface is saturated. During this time, only small amounts of chlorine-containing products are detected in the reactor effluent. After this initial period of operation, Cl-containing compounds, including HCl, Cl₂ and COCl₂ are evolved from the surface.

Recommendations

Based on the research described in this report, the following recommendations are made for further investigation:

- The hypothesis that the lack of carbon mass balance closure under some conditions was due to undetected/unidentified volatile partial oxidation intermediates should be tested.
- The preferred PCO reactor Configuration 2 should be tested at an acceptable field site so that the objectives related to practical

integration of PCO with air stripping, and perhaps vacuum soil vapor extraction can be achieved.

- First principles modeling of the preferred PCO reactor configuration should be undertaken to allow reactor optimization to be performed in a rapid, efficient and scientifically sound manner. The modeling effort should include submodels for the UV radiation field and intrinsic VOC destruction rate expressions, as well as the reactor-scale advection-diffusion-reaction model.
- Testing efforts should be focused on sites that are contaminated with chlorinated ethylenes. Avoid sites contaminated with such recalcitrant compounds as aromatics and chlorinated ethanes.
- Equipment development efforts should continue to focus on advanced reactor designs. Based on previous experience, it is likely that a large margin for process performance improvement exists through this avenue.

The full report was submitted in fulfillment of contract number CR 821100-01-0 by Arizona State University under the sponsorship of the United States Environmental Protection Agency. The report covers a period from October 1, 1993, to June 30, 1997, and work was completed as of June 30, 1997.

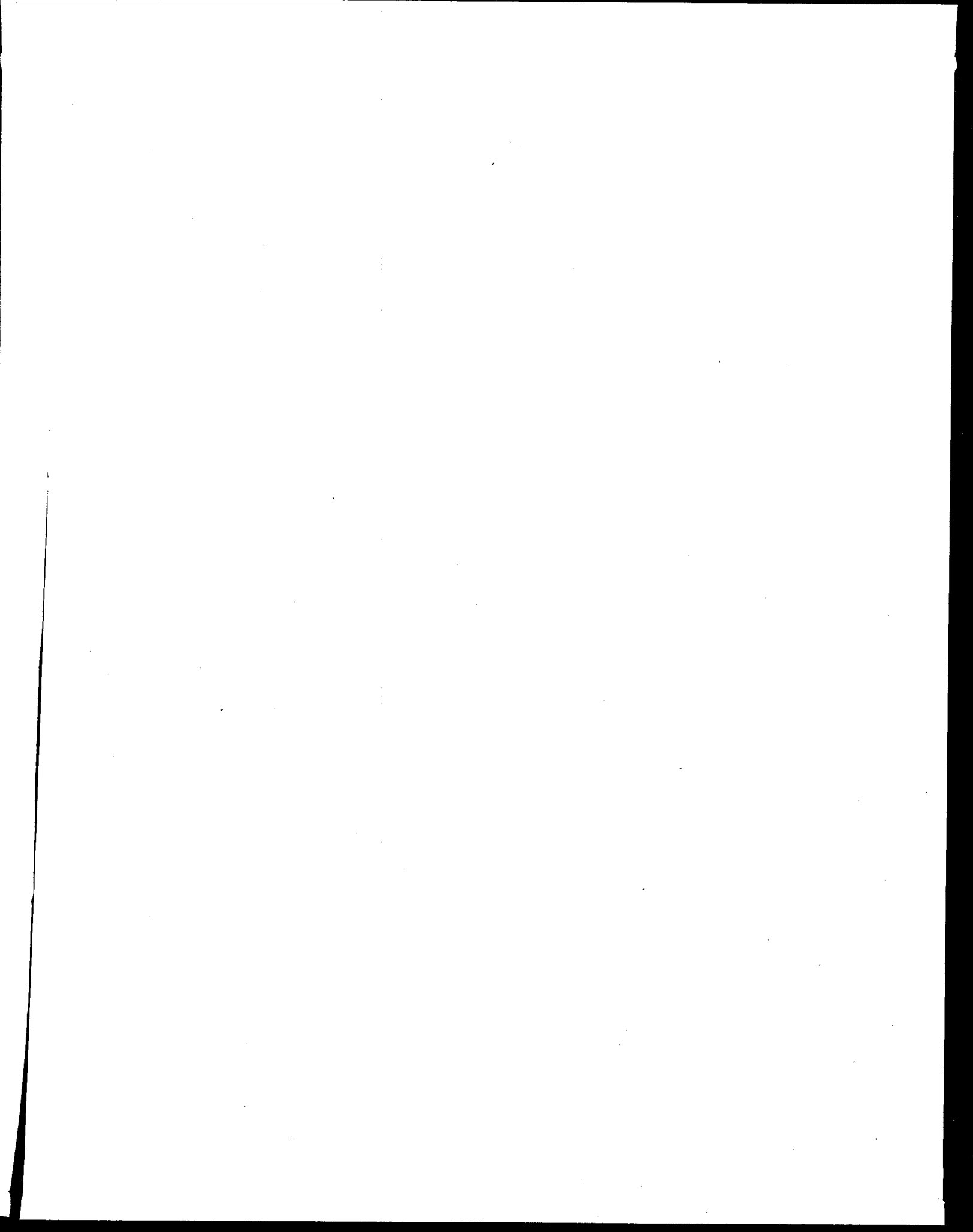
Rajnish Changrani and Gregory B. Raupp are with Arizona State University, Tempe, AZ 85287-6006. Craig Turchi is with NEPCCO Environmental Systems, Ocala, FL 34470.

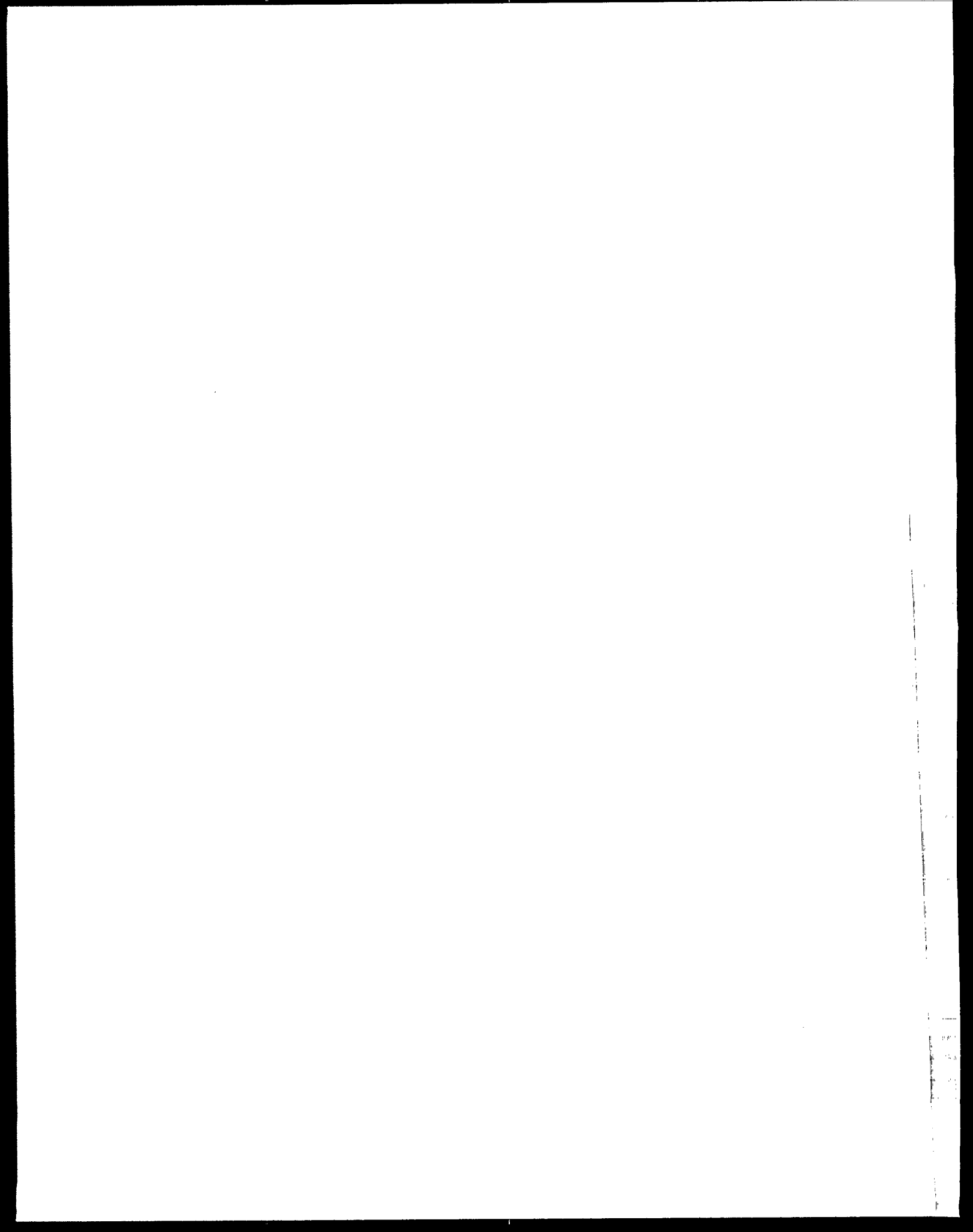
Norma M. Lewis is the EPA Project Officer (see below).

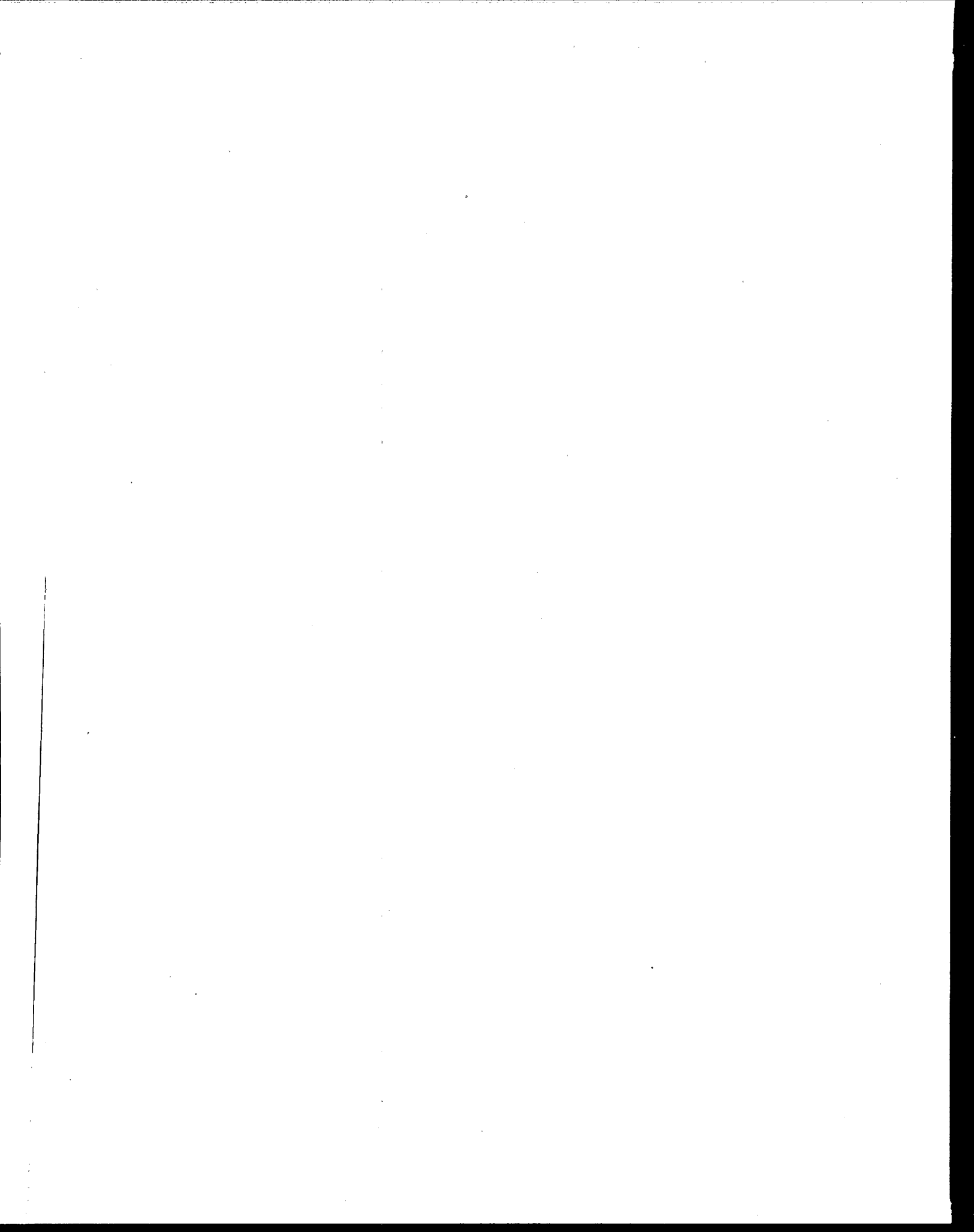
The complete report, entitled "Integration of Photocatalytic Oxidation with Air Stripping of Contaminated Aquifers," (Order No. PB99-127920; Cost: \$25.50, subject to change) will be available only from:

*National Technical Information Service
5285 Port Royal Road
Springfield, VA 22161
Telephone: 703-605-6000*

*The EPA Project Officer can be contacted at:
National Risk Management Research Laboratory
U.S. Environmental Protection Agency
Cincinnati, OH 45268*







United States
Environmental Protection Agency
Center for Environmental Research Information
Cincinnati, OH 45268

Please make all necessary changes on the below label,
detach or copy, and return to the address in the upper
left-hand corner.

If you do not wish to receive these reports CHECK HERE ;
detach, or copy this cover, and return to the address in the
upper left-hand corner.

PRESORTED STANDARD
POSTAGE & FEES PAID
EPA
PERMIT No. G-35

Official Business
Penalty for Private Use
\$300

EPA/540/SR-98/504